Nanoscale

PAPER

View Article Online
View Journal | View Issue

Cite this: *Nanoscale*, 2020, **12**, 21218

COF-inspired fabrication of two-dimensional polyoxometalate based open frameworks for biomimetic catalysis†

Yu Zhao,‡[a] Zhifang Wang,‡[a] Jia Gao,[a] Zhengfeng Zhao,[d] Xia Li,[a] Ting Wang,[a] Peng Cheng,[a,b,c] Shengqian Ma,[e] Yao Chen *[a,d] and Zhenjie Zhang *[a,b,c]

The development of highly efficient and robust biomimetic catalysts is an essential and feasible strategy to overcome the intrinsic drawbacks of natural enzymes. Inspired by the synthetic strategy of covalent organic frameworks, we adopted a covalent-bond-driven strategy to prepare polyoxometalate (POM) based open frameworks (NKPOM-OFs = Nankai University POM-OFs) with abundant Mo═O groups that can mimic the active center of sulfite oxidase. Four 2-dimensional (2D) NKPOM-OFs were designed and synthesized *via* the condensation reaction of linear amino-containing POMs with planar tetra-aldehyde monomers. Benefitting from the high crystallinity, the structures of 2D POM-OFs can be successfully determined from structural simulations. The results unveiled that NKPOM-OFs possessed 2D staggered stacking layered structures with the **sql** topology. All these NKPOM-OFs exhibited high crystallinity and stability and demonstrated outstanding performance to serve as biomimetic catalysts of sulfite oxidase with good recyclability. Notably, exfoliation of NKPOM-OFs under ultrasonic treatment can significantly boost the catalytic activity with almost two times faster reaction rates. This study not only enriches the facile and versatile synthesis strategy for POM-OFs but also provides new biomimetic platforms for biocatalysis.

Received 31st July 2020,
Accepted 20th September 2020

DOI: 10.1039/d0nr05662f

rsc.li/nanoscale

Introduction

Natural enzymes have demonstrated great potential in the applications of many fields as diverse as pharmaceutical processes, food industry, biosensing, *etc.*, which is attributed to their extraordinary and unique catalytic properties, such as ultrahigh efficiency and remarkable regio-/stereo-selectivity.[1,2] However, some intrinsic drawbacks such as high cost, low stability, and recyclability have handicapped their practical applications.[3] Besides the direct modification of enzymes, the development of effective and robust biomimetic catalysts has been emerging as an essential and feasible strategy to tackle the aforementioned problems.[4,5] A rational design approach is to mimic the structural features of natural enzymes, *i.e.*, design complexes or materials possessing a similar structure to that of active centers in enzymes.[6] Sulfite oxidase is an essential eukaryotic molybdenum enzyme that can oxidize sulfite to sulfate.[7] In animal cells, the oxidation of sulfur-containing amino acids usually leads to the formation of sulfite and is further converted to nontoxic sulfate through oxidation, fulfilled by sulfite oxidase. Therefore, this enzyme is of great importance as it is involved in the last step of detoxification of sulfur in cells. The active center of sulfite oxidase contains two Mo═O groups, which can oxidize sulfite to sulfate[8] accompanied by a reduction of Mo(VI) to Mo(IV). Currently, fabrication of biomimetic materials that can mimic the structure and function of sulfite oxidase has rarely been reported, and most of the related studies focus on molybdenum oxide and molybdenum coordination complexes.[9–13] For example, Yang *et al.* prepared PEGylated molybdenum oxide nanoparticles to mimic sulfite oxidase for vitamin B1 detection.[13] However, challenges remain in terms of the improvement of catalytic performance and the construction of diverse biomimetic catalysts. For instance, the design of porous networks is desirable

[a]*State Key Laboratory of Medicinal Chemical Biology, College of Chemistry, Nankai University, Tianjin 300071, China*
[b]*Renewable Energy Conversion and Storage Center, Nankai University, Tianjin 300071, China*
[c]*Key Laboratory of Advanced Energy Materials Chemistry, Ministry of Education, Nankai University, Tianjin 300071, China*
[d]*College of Pharmacy, Nankai University, Tianjin 300071, China. E-mail: chenyao@nankai.edu.cn, zhangzhenjie@nankai.edu.cn*
[e]*Department of Chemistry, University of North Texas 1508 W Mulberry St, Denton, TX 76201, USA*

†Electronic supplementary information (ESI) available. CCDC 1997411 and 1997412. For ESI and crystallographic data in CIF or other electronic format see DOI: 10.1039/d0nr05662f

‡These authors contributed equally to this work.

for highly efficient catalysts, because they can facilitate the substrate/product mass transfer; fabrication of 2-dimensional (2D) layered structures that can be exfoliated into nanosheets is crucial to maximize the accessible catalytic sites for the enhancement of catalytic efficiency. Moreover, heterogeneous catalysts are conducive to the recycling of the catalysts and the purification of the product as they can be easily separated from the catalytic system by centrifugation or filtration.

Polyoxometalates (POMs) are anionic metal oxides composed of transition metals especially molybdenum.[14–25] The abundant Mo═O groups in POMs possess high structural similarity to the catalytic centers of sulfite oxidase. Thus, application of POMs as building blocks to construct POM-based open frameworks (POM-OFs) would be a facile and ideal approach to fabricate biomimetic catalysts of sulfite oxidase due to their advantages such as robustness, intrinsic porosity, easy to recycle, *etc*.[26–28] Currently, the traditional strategy to construct POM-OFs is mainly based on coordination-bond-driven synthesis (Scheme 1).[29–33] Nitrogen and oxygen-donor ligands are frequently used as organic linkers to connect with POMs *via* coordination bonds.[34,35] However, due to the complicated and variable coordination modes of POMs, it is challenging to precisely control and predict the final structures and functions of POM-OFs.[36] Therefore, the design and synthesis of POM-OFs with desirable networks are of considerable significance and in high demand. Covalent organic frameworks (COFs) are a class of fully pre-designable polymeric materials which is composed of geometrically predefined building blocks.[37–44] The crystallinity of COFs mostly relies on the reversible linkage dynamics (*e.g.*, reversible imine bonds), and the structures of COFs can be determined by powder X-ray diffraction (PXRD) and electron diffraction tomography (EDT) assisted with computational simulation. Covalent bonding has been proved to be an efficient approach to construct POM hybrids.[45] Recently, Yaghi and other groups reported a series of three-dimensional (3D) POM-OFs synthesized by linking amino functionalized polyoxometalate with 4-connected aldehyde building units through imine condensation.[46–48] Herein, we expanded the covalent-bond-driven synthesis strategy to construct two-dimensional (2D) POM-OFs with targeted topologies (Scheme 1). A series of NKPOM-OFs (Nankai University POM-OFs) with high crystallinity and robustness were designed and developed as biomimetic catalysts of sulfite oxidase that demonstrate high catalytic efficiency and reusability.

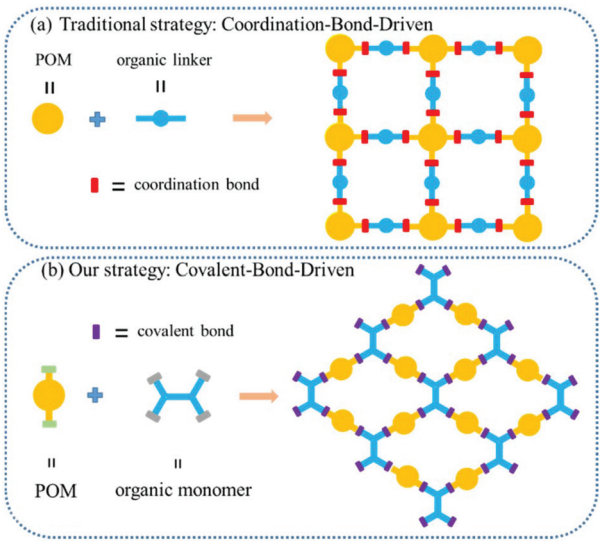

Scheme 1 Illustration of the traditional 'Coordination-Bond-Driven' synthesis strategy (upper), and the new 'Covalent-Bond-Driven' synthesis strategy of POM-OFs (bottom).

Results and discussion

Synthesis and characterization of NKMOP-OFs

To demonstrate proof of concept, we first chose an Anderson-type POM containing two active amino groups, $[N(C_4H_9)_4]_3[CoMo_6O_{18}\{(OCH_2)_3CNH_2\}_2]$ (named **$CoMo_6$**), as the building block and applied the imine bond as the linkage.[49–51] The amino-functionalized **$CoMo_6$** POM can serve as a rigid and linear building block with two active amino groups located on the opposite positions. In order to analyze the reactivity and structural intactness of **$CoMo_6$**, a model compound (**MC-Co**) was first prepared *via* a condensation reaction of benzaldehyde with **$CoMo_6$** (Fig. 1a). The molecular structure of **MC-Co** was successfully unveiled by Single Crystal X-Ray Diffraction (SCXRD) that revealed that the **$CoMo_6$** core was connected with two coplanar phenyl groups *via* C═N bonds. The bond length of C═N is ~1.3 Å, indicating its double bond characteristic. The formation of imine bonds was further confirmed by Fourier-transform infrared (FT-IR) spectroscopy (Fig. 1b). The appeared stretching bands at 1638 cm^{-1} of **MC-Co** confirmed the formation of imine bonds. The ^1H NMR, ^{13}C NMR, DEPT-135 (distortionless enhancement by polarization transfer) and 2D ^{13}C-^1H HSQC (heteronuclear single quantum correlation) spectra were also recorded to investigate the chemical components of **MC-Co** (Fig. S1–S4†). The peaks

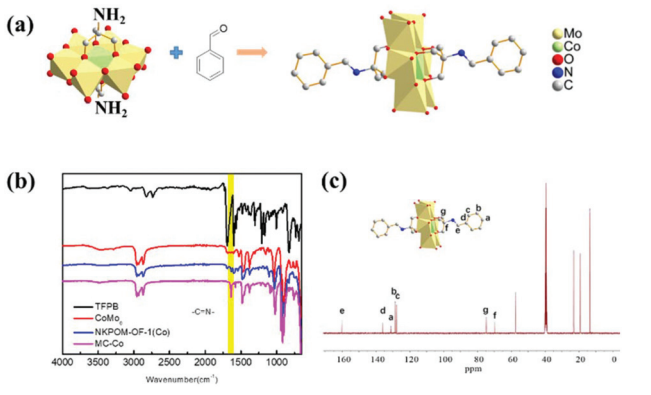

Fig. 1 (a) Synthetic route and crystal structure of **MC-Co**. H atoms are omitted for clarity. (b) FT-IR spectra of TFPB, **$CoMo_6$**, **NKPOM-OF-1(Co)** and **MC-Co**. (c) ^{13}C NMR spectrum of **MC-Co**.

at 8.36 ppm in ^{1}H NMR and 160.15 ppm in ^{13}C NMR are corresponding to the characteristic signals of the imine group (Fig. 1c and S1†). These results validated the high reactivity and structural intactness of POM monomers during the condensation reaction process and indicated that **$CoMo_6$** could be an ideal POM building block to construct POM-OFs *via* the covalent-bond-driven approach.

Up to now, most COFs possess 2D layered structures with specific topologies (*e.g.* **sql**, **hcb**, and **kgm**) because a combination of planar building blocks can easily restrict the growth of the polymer backbones in a 2D manner. Over the past decades, 2D materials have attracted great attention due to their remarkable advantages. For instance, 2D materials can be exfoliated to nanosheets that expose more catalytic sites to boost the catalytic activity. Moreover, the structures of 2D materials can be feasibly determined *via* PXRD and High-Resolution Transmission Electron Microscopy (HR-TEM). In order to realize the construction of POM-OFs *via* the covalent-bond-driven approach, we designed a planar tetra-aldehyde monomer, 1,2,4,5-tetrakis-(4-formylphenyl)benzene (TFPB), to react with **$CoMo_6$** in a solution mixture of 1,4-dioxane and acetic acid at 120 °C for 3 days that afforded a green powder of **NKPOM-OF-1(Co)** (Fig. 2a). FT-IR spectra (Fig. 1b) showed the appearance of the stretching bands at 1635 cm^{-1}, indicating the formation of imine bonds in **NKPOM-OF-1(Co)**. We further explored the chemical components of **NKPOM-OF-1(Co)** through solid-state ^{13}C NMR spectroscopy. The characteristic peak at 160 ppm corresponds to the imine bond (Fig. 2b). The peaks between 125 and 150 ppm can be assigned to phenyl rings. The peaks at 57, 24, 20, and 14 ppm can be assigned to the signals of tetrabutylammonium (TBA) counterions. In addition, the charateristic peaks of the aldehyde were attenuated in IR and ^{13}C NMR spectra, indicating the high polymerization degrees of NKPM-OFs. Benefitting from the similarity of NKPOM-OFs to COF systems, we were able to determine their structure by analyzing PXRD data (Fig. 2c). The PXRD pattern of **NKPOM-OF-1(Co)** showed an intense peak at 2θ = 6.5°, which can be assigned to the (021) plane. The peaks at 2θ = 9.3 and 11.3° correspond to the (002) and (202) planes, respectively. The experimental pattern of **NKPOM-OF-1(Co)** matched well with the simulated pattern of the staggered stacking model (2D network with the **sql** topology). Pawley refinement yielded a unit cell of a = 26.40 Å, b = 39.00 Å, c = 19.00 Å, α = 90.1°, β = 88.2°, γ = 90.0° with R_{wp} = 2.57% and R_p = 1.91%. In addition, it was found that **NKPOM-OF-1(Co)** showed good stability in solvents, including water, DMSO, DMF, and methanol, confirmed by PXRD data (Fig. S6†).

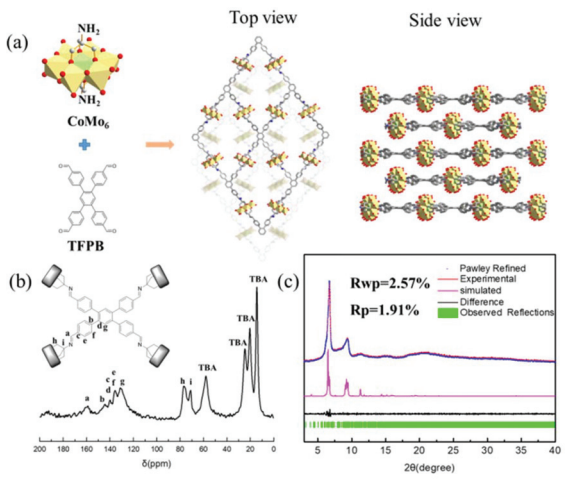

Fig. 2 (a) The synthetic route of **NKPOM-OF-1(Co)**. (b) ^{13}C CP/MAS NMR data of **NKPOM-OF-1(Co)**. (c) PXRD patterns of **NKPOM-OF-1(Co)**.

To further study the morphology of **NKPOM-OF-1(Co)**, scanning electron microscopy (SEM) images were collected. SEM images showed that **NKPOM-OF-1(Co)** particles are of block shape (~2 μm) (Fig. S7†). Energy-dispersive X-ray spectroscopy (EDX) mapping proved that **NKPOM-OF-1(Co)** was constructed from **$CoMo_6$** POMs, indicated by the existence of Mo and Co (Fig. S8†). N_2 sorption at 77 K was conducted to evaluate the porosity of **NKPOM-OF-1(Co)** (Fig. S9†). It was found that the surface area is relatively low (Langmuir surface area: 134 m^2 g^{-1}). The relatively low surface area could be due to the staggered stacking model and the existence of TBA counterions that partially blocked the pores. The same phenomenon has been reported in the literature.[52,53] We also calculated the theoretical surface area using the Material Studio software (Table S1†) and found that the calculated surface area matched well with the experimental result.

Exploration of the generality of the covalent-bond-driven approach

To analyze the generality of the new strategy to fabricate POM-OFs, we introduced another POM monomer, $[N(C_4H_9)_4]_3[MnMo_6O_{18}\{(OCH_2)_3CNH_2\}_2]$ (**$MnMo_6$**), which has a similar molecular structure to that of **$CoMo_6$**. A model compound, **MC-Mn**, was also successfully prepared *via* the reaction of benzaldehyde with **$MnMo_6$**, confirmed by SCXRD, FTIR, and NMR data (Fig. S10–S12†). As predicted, the reaction of **$MnMo_6$** with TFPB also afforded a 2D isostructural POM-OF of **NKPOM-OF-1(Co)** and **NKPOM-OF-1(Mn)**, confirmed by PXRD data (Fig. S13†). The SEM images showed blocky particles with a size of ~1 μm (Fig. S14†).

Besides POM building blocks, we also designed another 4-connected planar aldehyde monomer, 4,4′,4″,4‴-(ethene-1,1,2,2-tetrayl)tetrabenzaldehyde (ETTBA). A reaction of ETTBA with **$CoMo_6$** and **$MnMo_6$** afforded **NKPOM-OF-2(Co)** and **NKPOM-OF-2(Mn)**, respectively. The FT-IR and ^{13}C NMR spectra were used to study the formation of imine bonds (Fig. S15–S18†). PXRD analysis revealed that **NKPOM-OF-2(Co)** and **NKPOM-2(Mn)** also possessed a similar network to that of **NKPOM-OF-1(Co)** with a 2D network of the **sql** topology (Fig. 3a). For **NKPOM-OF-2(Mn)** and **NKPOM-OF-2(Co)**, the space group was determined as $P2$ with a = 35.04 Å, b = 28.30 Å, c = 19.01 Å, $\alpha = \gamma$ = 90.0°, and β = 87.4°. The Pawley-refined patterns matched well with the experimental data (Fig. 3b and S19†). HR-TEM showed distinct lattice fringes of **NKPOM-OF-2(Co)** that confirmed its high crystallinity and

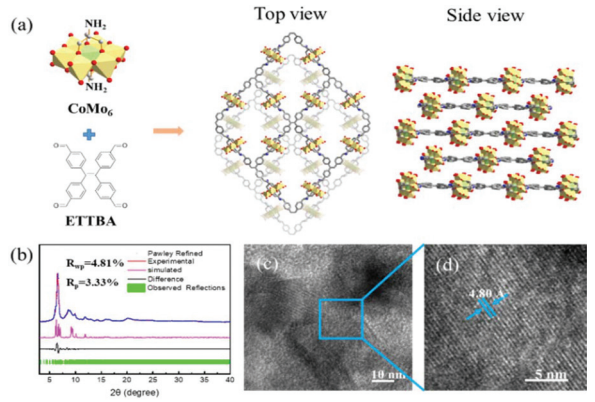

Fig. 3 (a) The synthetic route of **NKPOM-OF-2(Co)**. (b) PXRD patterns of **NKPOM-OF-2(Co)**. (c) HR-TEM image of **NKPOM-OF-2(Co)**. (d) Partial enlarged details of (c).

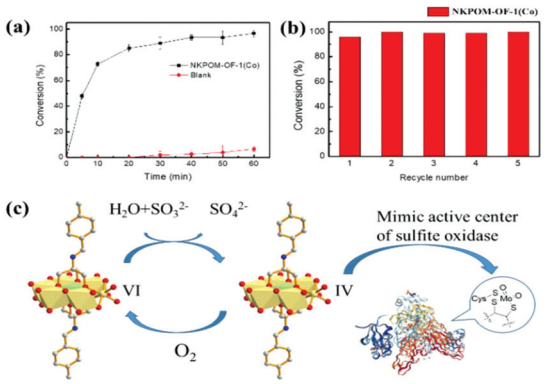

Fig. 4 (a) Conversion of sulfite to sulfate catalyzed by **NKPOM-OF-1(Co)**. Reaction conditions: Na_2SO_3 (6.6 mM), **NKPOM-OF-1(Co)** (1 mg mL^{-1}). (b) Recycling experiments of **NKPOM-OF-1(Co)**. Reaction conditions: Na_2SO_3 6.6 (mM), **NKPOM-OF-1(Co)** (1 mg mL^{-1}), time (60 min). (c) The proposed mechanism of **NKPOM-OF-1(Co)** mimicking sulfite oxidase.

layered structure (Fig. 3c, and d). The lattice fringes with a lattice spacing of 0.48 nm correspond to the (004) atomic plane. The SEM images showed similar morphologies for **NKPOM-OF-2(Mn)** and **NKPOM-OF-2(Co)** (Fig. S20†). TEM also revealed that the particles are the aggregation of microcrystals (Fig. S21†). EDX mapping indicated that NKPOM-OFs contained all the expected elements (Fig. S22–S24†). N_2 sorption at 77 K showed similar profiles with hysteresis in the desorption isotherm (Fig. S25–27†), possibly due to the pore connectivity effects according to literature results.[54] The Langmuir surface areas of **NKPOM-OF-1(Mn)**, **NKPOM-OF-2(Mn)**, and **NKPOM-OF-2(Co)** are 134 $m^2\ g^{-1}$, 212 $m^2\ g^{-1}$, and 226 $m^2\ g^{-1}$, respectively. For comparison, N_2 sorption at 77 K unveiled the nonporous nature of $MnMo_6$ and $CoMo_6$ (Fig. S28†). PXRD data revealed that NKPOM-OFs showed high stability in common solvents, including water (Fig. S29–S31†). NKPOM-OFs also showed high thermal stability (250 °C) according to TGA (Fig. S32–S34†). The properties can benefit the application of NKPOM-OFs for biocatalysis.

Evaluation of the biomimetic activity of NKMOP-OFs

The structure of two POM monomers is similar to that of active centers of sulfite oxidase. In sulfite oxidase, the molybdenum center was connected by three sulfur and two oxo ligands. During the catalysis, sulfite is bound to the equatorial oxo group of the Mo center, the oxo group is transformed into hydroxyl/water ligands and Mo(VI) turns into Mo(IV). In $MnMo_6$ and $CoMo_6$, there are three kinds of oxo groups: triply bridging oxygen from $H_2NC(CH_2O)_3$ residues, doubly bridging oxygen and terminal oxygen. The terminal oxygen group is similar to the equatorial oxo group of sulfite oxidase. Thus, we examined the sulfite oxidase activity of NKPOM-OFs by catalyzing the reaction of SO_3^{2-} to SO_4^{2-}. After the reaction, FT-IR spectra of the product confirmed the formation of SO_4^{2-} (Fig. S35†). As shown in Fig. 4a, a high conversion (>95%) was observed in 60 min for **NKPOM-OF-1(Co)**, while the blank reaction afforded a much lower conversion (<10%). The calculation based on the conversion in 5 min revealed that the turnover number (TON) and turnover frequency (TOF) were 7 and 1.4 min^{-1}, respectively, for **NKPOM-OF-1(Co)**. Although the TOF is lower than that of the natural sulfite oxidase (Table S2†), the heterogeneous system makes it easy to reuse **NKPOM-OF-1(Co)**. It could be recycled for at least 5 times without any loss in conversion efficiency (Fig. 4b). We also found that **NKPOM-OF-1(Mn)**, **NKPOM-OF-2(Co)**, and **NKPOM-OF-2(Mn)** showed high catalytic activity (>95%) and excellent recyclability (Fig. S36–S41†). PXRD patterns showed that NKPOM-OFs maintained their crystallinity after recycling experiments (Fig. S42–S43†), further indicating the heterogeneous nature of NKPOM-OFs. Although the model compound and POM monomers also showed similar catalytic activity (Fig. S44†), the homogeneous catalytic systems were difficult to recycle that limited their applications. The mechanism of the catalysis reaction was investigated to interpret the catalytic performance of NKPOM-OFs. It is well known that POMs can catalyze the oxidations of substrates, and the reduced POMs could be reoxidized by O_2.[55] Thus, we proposed that the sulfite was oxidized into sulfate while Mo(VI) transformed into Mo(IV) which can be reoxidized by O_2 in the air to complete the cycle (Fig. 4c). To support this hypothesis, we examined the catalytic activity under O_2 or Ar atmospheres as comparisons. The conversion of sulfite can reach >99% in as short as 10 min under an O_2 atmosphere, while the conversion reduced to <9% under an Ar atmosphere even after extending the reaction time to 30 min (Fig. S45†). These results strongly supported our hypothesis and revealed that O_2 played a critical role in this catalytic system.

Considering the low porosity of NKPOM-OF, we thought that the catalytic reaction mostly took place on materials' surface. Thus, exfoliation of 2D materials to form nanosheets would expose more active sites to boost catalytic performance.[56] In order to further improve the catalytic efficiency of NKPOM-OFs, we attempted to exfoliate NKPOM-OFs into nanosheets. After supersonic treatment, the exfoliated

NKPOM-OFs (named NKPOM-OF-e) were investigated by TEM, which showed sheet structures after exfoliation (Fig. S43†). Atomic Force Microscopy (AFM) revealed that the thickness of NKPOM-OF-e was about 1.2 nm (Fig. S46–48†). Dynamic light scattering (DLS) data indicated that the diameter of NKPOM-OF-e particles is among hundreds of nanometers (Fig. S49–S52†). The crystallinity of exfoliated structures was also checked by PXRD patterns (Fig. S53†), indicating that all materials maintained their crystallinity after exfoliation. The FT-IR spectra of four NKPOM-OFs also showed no change before and after exfoliation, which suggested that the imine-linked network was conserved (Fig. S54†). We then evaluated their biomimetic activity of sulfite oxidase and found that their activity was significantly boosted (conversion >95% in 30 min). The reaction rates were almost two times faster than those of bulk NKPOM-OFs (Fig. S55†). ICP-OES (inductively coupled plasma-optical emission spectrometry) and UV analysis proved no leaching of POM monomers from NKPOM-OF-e, indicating that NKPOM-OF-e remained intact during the catalytic reaction.

Conclusions

In summary, we reported four NKPOM-OFs as biomimetic catalysts synthesized *via* the covalent-bond-driven approach. To demonstrate proof of concept, we chose an amino-containing Anderson-type POM as the linear building blocks of POM-OFs. Single crystal structure data of discrete model compounds formed by the reaction of benzaldehyde and POM monomers unveiled the high reactivity and structural intactness of POMs. Hence, an imine condensation reaction of POMs with planar tetra-aldehyde monomers afforded four 2D NKPOM-OFs with high crystallinity and outstanding stability. Notably, learned from the structure determination methods of COFs by analyzing PXRD and HR-TEM data, the structures of NKPOM-OFs were determined to be 2D layered networks with the **sql** topology. Structural analysis revealed that Mo═O groups in NKPOM-OFs showed high similarity to the active centers of sulfite oxidase. Thus, NKPOM-OFs can serve as highly efficient catalysts to mimic the activity of sulfite oxidase as they can integrate the advantages of both POMs and COFs: high catalytic efficiency of POMs; excellent stability of covalent linkages inherited from COFs; enhanced mass transfer of the porous framework; and easy to recycle due to their heterogeneous nature. Furthermore, we employed an exfoliation strategy to fabricate nanosheets of NKPOM-OFs that dramatically boosted their catalytic efficiency. This study paves a new avenue to fabricate functional POM-OFs and provides a new methodology for structural determination of POM-OFs.

Conflicts of interest

There are no conflicts to declare.

Acknowledgements

The authors acknowledge the financial support from the National Natural Science Foundation of China (21871153 and 31800793), the 111 Project (B12015) and the Postdoctoral Science Foundation of China (2019M660974). The authors also thank Professor Zhaoyong Lu for his helpful discussions regarding the NMR experiments.

Notes and references

1 R. Wolfenden and M. J. Snider, The depth of chemical time and the power of enzymes as catalysts, *Acc. Chem. Res.*, 2001, **34**, 938–945.
2 Y. Lin, J. Ren and X. Qu, Catalytically active nanomaterials: A promising candidate for artificial enzymes, *Acc. Chem. Res.*, 2014, **47**, 1097–1105.
3 J. Wu, X. Wang, Q. Wang, Z. Lou, S. Li, Y. Zhu, L. Qin and H. Wei, Nanomaterials with enzyme-like characteristics (nanozymes): next-generation artificial enzymes (II), *Chem. Soc. Rev.*, 2019, **48**, 1004–1076.
4 R. Ragg, M. N. Tahir and W. Tremel, Solids go bio: Inorganic nanoparticles as enzyme mimics, *Eur. J. Inorg. Chem.*, 2016, **13–14**, 1906–1915.
5 Y. Lin, J. Ren and X. Qu, Nano-gold as artificial enzymes: Hidden talents, *Adv. Mater.*, 2014, **26**, 4200–4217.
6 T. R. Simmons, G. Berggren, M. Bacchi, M. Fontecave and V. Artero, Mimicking hydrogenases: From biomimetics to artificial enzymes, *Coord. Chem. Rev.*, 2014, **270–271**, 127–150.
7 G. Schwarz, R. R. Mendel and M. W. Ribbe, Molybdenum cofactors, enzymes and pathways, *Nature*, 2009, **460**, 839–847.
8 R. Hille, The reaction mechanism of oxomolybdenum enzymes, *Biochim. Biophys. Acta*, 1994, **1184**, 143–169.
9 J. Mitra and S. Sarkar, Oxo-Mo(IV)(dithiolene)thiolato complexes: analogue of reduced sulfite oxidase, *Inorg. Chem.*, 2013, **52**, 3032–3042.
10 M. L. Mader, M. D. Carducci and J. H. Enemark, Analogues for the molybdenum center of sulfite oxidase: oxomolybdenum(V) complexes with three thiolate sulfur donor atoms, *Inorg. Chem.*, 2000, **39**, 525–531.
11 K. Peariso, B. S. Chohan, C. J. Carrano and M. L. Kirk, Synthesis and EPR characterization of new models for the one-electron reduced molybdenum site of sulfite oxidase, *Inorg. Chem.*, 2003, **42**, 6194–6203.
12 R. Ragg, F. Natalio, M. N. Tahir, H. Janssen, A. Kashyap, D. Strand, S. Strand and W. Tremel, Molybdenum trioxide nanoparticles with intrinsic sulfite oxidase activity, *ACS Nano*, 2014, **8**, 5182–5189.
13 Y. Chen, T. Chen, X. Wu and G. Yang, Oxygen vacancy–engineered PEGylated MoO3−x nanoparticles with superior sulfite oxidase mimetic activity for vitamin B1 detection, *Small*, 2019, **15**, 1903153.

14 D. L. Long, E. Burkholder and L. Cronin, Polyoxometalate clusters, nanostructures and materials: From self-assembly to designer materials and devices, *Chem. Soc. Rev.*, 2007, **36**, 105–121.
15 A. Blazevic and A. Rompel, The Anderson-Evans polyoxometalate: From inorganic building blocks via hybrid organic–inorganic structures to tomorrows "Bio-POM", *Coord. Chem. Rev.*, 2016, **307**, 42–64.
16 J. Zhang, Y. Huang, G. Li and Y. Wei, Recent advances in alkoxylation chemistry of polyoxometalates: From synthetic strategies, structural overviews to functional applications, *Coord. Chem. Rev.*, 2019, **378**, 395–414.
17 H. Tan, Y. Li, Z. Zhang, C. Qin, X. Wang, E. Wang and Z. Su, Chiral polyoxometalate-induced enantiomerically 3D architectures: A new route for synthesis of high-dimensional chiral compounds, *J. Am. Chem. Soc.*, 2007, **129**, 10066–10067.
18 Y. Song and R. Tsunashima, Recent advances on polyoxometalate-based molecular and composite materials, *Chem. Soc. Rev.*, 2012, **41**, 7384–7402.
19 A. Dolbecq, E. Dumas, C. R. Mayer and P. Mialane, Hybrid organic-inorganic polyoxometalate compounds: From structural diversity to applications, *Chem. Rev.*, 2010, **110**, 6009–6048.
20 P. Yin, D. Li and T. Liu, Solution behaviors and self-assembly of polyoxometalates as models of macroions and amphiphilic polyoxometalate-organic hybrids as novel surfactants, *Chem. Soc. Rev.*, 2012, **41**, 7368–7383.
21 J. J. Walsh, A. M. Bond, R. J. Forster and T. E. Keyes, Hybrid polyoxometalate materials for photo(electro-) chemical applications, *Coord. Chem. Rev.*, 2016, **306**, 217–234.
22 B. Qin, H. Chen, H. Liang, L. Fu, X. Liu, X. Qiu, S. Liu, R. Song and Z. Tang, Reversible photoswitchable fluorescence in thin films of inorganic nanoparticle and polyoxometalate assemblies, *J. Am. Chem. Soc.*, 2010, **132**, 2886–2888.
23 A. Proust, B. Matt, R. Villanneau, G. Guillemot, P. Gouzerh and G. Izzet, Functionalization and post-functionalization: a step towards polyoxometalate-based materials, *Chem. Soc. Rev.*, 2012, **41**, 7605–7622.
24 H. Lv, Y. Geletii, C. Zhao, J. W. Vickers, G. Zhu, Z. Luo, J. Song, T. Lian, D. G. Musaev and C. L. Hill, Polyoxometalate water oxidation catalysts and the production of green fuel, *Chem. Soc. Rev.*, 2012, **41**, 7572–7589.
25 H. Lv, W. Guo, K. Wu, Z. Chen, J. Bacsa, D. G. Musaev, Y. V. Geletii, S. M. Lauinger, T. Lian and C. L. Hill, A noble-metal-free, tetra-nickel polyoxotungstate catalyst for efficient photocatalytic hydrogen evolution, *J. Am. Chem. Soc.*, 2014, **136**, 14015–14018.
26 I. Nath, J. Chakraborty and F. Verpoort, Metal organic frameworks mimicking natural enzymes: a structural and functional analogy, *Chem. Soc. Rev.*, 2016, **45**, 4127–4170.
27 H. N. Miras, L. Vilà-Nadal and L. Cronin, Polyoxometalate based open-frameworks (POM-OFs), *Chem. Soc. Rev.*, 2014, **43**, 5679–5699.
28 X. X. Li, D. Zhao and S. T. Zheng, Recent advances in POM-organic frameworks and POM-organic polyhedral, *Coord. Chem. Rev.*, 2019, **397**, 220–240.
29 X. X. Li, Y. X. Wang, R. H. Wang, C. Y. Cui, C. B. Tian and G. Y. Yang, Designed assembly of heterometallic cluster organic frameworks based on Anderson–type polyoxometalate clusters, *Angew. Chem., Int. Ed.*, 2016, **55**, 6462–6466.
30 Q. Han, C. He, M. Zhao, B. Qi, J. Niu and C. Duan, Engineering chiral polyoxometalate hybrid metal-organic frameworks for asymmetric dihydroxylation of olefins, *J. Am. Chem. Soc.*, 2013, **135**, 10186–10189.
31 Y. J. Chen, X. Huang, Y. Chen, Y. R. Wang, H. Zhang, C. X. Li, L. Zhang, H. Zhu, R. Yang, Y. H. Kan, S. L. Li and Y. Q. lan, Polyoxometalate-induced efficient recycling of waste polyester plastics into metal-organic frameworks, *CCS Chem.*, 2019, **1**, 561–570.
32 J. Song, Z. Luo, D. K. Britt, H. Furukawa, O. M. Yaghi, K. I. Hardcastle and C. L. Hill, A multiunit catalyst with synergistic stability and reactivity: A polyoxometalate-metal organic framework for aerobic decontamination, *J. Am. Chem. Soc.*, 2011, **133**, 16839–16846.
33 J. X. Liu, X. B. Zhang, Y. L. Li, S. L. Huang and G. Y. Yang, Polyoxometalate functionalized architectures, *Coord. Chem. Rev.*, 2020, **414**, 213260.
34 S. Taleghani, M. Mirzaei, H. Eshtiagh-Hosseini and A. Frontera, Tuning the topology of hybrid inorganic-organic materials based on the study of flexible ligands and negative charge of polyoxometalates: A crystal engineering perspective, *Coord. Chem. Rev.*, 2016, **309**, 84–106.
35 D. Y. Du, J. S. Qin, S. L. Li, Z. M. Su and Y. Q. Lan, Recent advances in porous polyoxometalate-based metal-organic framework materials, *Chem. Soc. Rev.*, 2014, **43**, 4615–4632.
36 D. Li, P. Ma, J. Niu and J. Wang, Recent advances in transition-metal-containing Keggin-type polyoxometalate-based coordination polymers, *Coord. Chem. Rev.*, 2019, **392**, 49–80.
37 K. Wang, D. Qi, Y. Li, T. Wang, H. Liu and J. Jiang, Tetrapyrrole macrocycle based conjugated two-dimensional mesoporous polymers and covalent organic frameworks: From synthesis to material applications, *Coord. Chem. Rev.*, 2019, **378**, 188–206.
38 R. P. Bisbey and W. R. Dichtel, Covalent organic frameworks as a platform for multidimensional polymerization, *ACS Cent. Sci.*, 2017, **3**, 533–543.
39 S. Y. Ding and W. Wang, Covalent organic frameworks (COFs): from design to applications, *Chem. Soc. Rev.*, 2013, **42**, 548–568.
40 X. Feng, X. Ding and D. Jiang, Covalent organic frameworks, *Chem. Soc. Rev.*, 2012, **41**, 6010–6022.
41 J. L. Segura, M. J. Mancheño and F. Zamora, Covalent organic frameworks based on Schiff-base chemistry: synthesis, properties and potential applications, *Chem. Soc. Rev.*, 2016, **45**, 5635–5671.
42 P. J. Waller, F. Gándara and O. M. Yaghi, Chemistry of covalent organic frameworks, *Acc. Chem. Res.*, 2015, **48**, 3053–3063.

43 S. Das, P. Heasman, T. Ben and S. Qiu, Porous organic materials: strategic design and structure-function correlation, *Chem. Rev.*, 2017, **117**, 1515–1563.
44 R. L. Liang, F. Z. Cui, R. H. A, Q. Y. Qi and X. Zhao, A Study on Constitutional Isomerism in Covalent Organic Frameworks: Controllable Synthesis, Transformation, and Distinct Difference in Properties, *CCS Chem.*, 2020, **2**, 139–145.
45 H. Wu, H. K. Yang and W. Wang, Covalently-linked polyoxometalate-polymer hybrids: optimizing synthesis, appealing structures and prospective applications, *New J. Chem.*, 2016, **40**, 886–897.
46 W. Xu, X. Pei, C. S. Diercks, H. Lyu, Z. Ji and O. M. Yaghi, A Metal-Organic Framework of Organic Vertices and Polyoxometalate Linkers as a Solid-State Electrolyte, *J. Am. Chem. Soc.*, 2019, **141**, 17522–17526.
47 X. Yu, C. Li, Y. Ma, D. Li, H. Li, X. Guan, Y. Yan, V. Valtchev, S. Qiu and Q. Fang, Crystalline, porous, covalent polyoxometalate-organic frameworks for lithium-ion batteries, *Microporous Mesoporous Mater.*, 2020, **299**, 110105.
48 R. Ma, N. Liu, T. T. Lin, T. Zhao, S. L. Huang and G. Y. Yang, Anderson polyoxometalate built-in covalent organic frameworks for enhancing catalytic performances, *J. Mater. Chem. A*, 2020, **8**, 8548–8553.
49 F. J. Uribe-Romo, J. R. Hunt, H. Furukawa, C. Klock, M. O'Keeffe and O. M. Yaghi, A Crystalline Imine-Linked 3-D Porous Covalent Organic Framework, *J. Am. Chem. Soc.*, 2009, **131**, 4570–4571.
50 S. K. Elsaidi, M. H. Mohamed, J. S. Loring, B. P. MaGrail and P. K. Thallapally, Coordination Covalent Frameworks: A New Route for Synthesis and Expansion of Functional Porous Materials, *ACS Appl. Mater. Interfaces*, 2016, **8**, 28424–28427.
51 H. L. Nguyen, F. Gándara, H. Furukawa, T. L. H. Doan, K. E. Cordova and O. M. Yaghi, A Titanium-Organic Framework as an Exemplar of Combining the Chemistry of Metal-and Covalent-Organic Frameworks, *J. Am. Chem. Soc.*, 2016, **138**, 4330–4333.
52 J. Zhang, T. Wu, S. Chen, P. Feng and X. Bu, Versatile Structure-Directing Roles of Deep-Eutectic Solvents and Their Implication in the Generation of Porosity and Open Metal Sites for Gas Storage, *Angew. Chem., Int. Ed.*, 2009, **48**, 3486–3490.
53 H. Fu, C. Chen, Y. Lu, Z. M. Zhang, Y. G. Li, Z. M. Su, W. L. Li and E. B. Wang, An Ionothermal Synthetic Approach to Porous Polyoxometalate-Based Metal-Organic Frameworks, *Angew. Chem., Int. Ed.*, 2012, **51**, 7985–7989.
54 M. Kruk and M. Jaroniec, Gas Adsorption Characterization of Ordered Organic-Inorganic Nanocomposite Materials, *Chem. Mater.*, 2001, **13**, 3169–3183.
55 I. A. Weinstock, R. E. Schreiber and R. Neumann, Dioxygen in polyoxometalate mediated reactions, *Chem. Rev.*, 2017, **118**, 2680–2717.
56 D. W. Burke, C. Sun, I. Castano, N. C. Flanders, A. M. Evans, E. Vitaku, D. C. McLeod, R. H. Lambeth, L. X. Chen, N. C. Gianneschi and W. R. Dichtel, Acid Exfoliation of Imine-linked Covalent Organic Frameworks Enables Solution Processing into Crystalline Thin Films, *Angew. Chem., Int. Ed.*, 2020, **59**, 5165–5171.